

THE ATHENS 1999 MAINSHOCK ($M_w=5.9$) AND THE EVOLUTION OF ITS AFTERSHOCK SEQUENCE

C.B. PAPAZACHOS¹, B.G. KARAKOSTAS¹, G.F. KARAKAISIS¹ AND CH.A. PAPAIOANNOU²

ABSTRACT

The spatial distribution of the aftershocks that followed the September 1999 mainshock ($M_w=5.9$), which caused severe damage and loss of life in the nearby city of Athens, is examined in the present work. P and S arrivals of seismic waves recorded by the permanent seismic network as well as by a number of digital seismographs and accelerographs, which had been deployed in the broader epicentral area shortly after the mainshock occurrence, were used for the determination of the focal parameters of the mainshock and its aftershocks. The spatial distribution of the aftershocks led to the recognition of the fault, which produced the September mainshock, while certain features of the rupture process may be deduced on the basis of their spatiotemporal variation.

KEY WORDS: Aftershock sequence, spatial and temporal aftershock distribution, normal faulting

1. FOCAL PARAMETERS OF THE SEPTEMBER 7, 1999 ($M_w=5.9$) ATHENS MAINSHOCK

The determination of the focal parameters of the mainshock was based on all the available P- and S- wave arrivals recorded at relatively small epicentral distances (P_g) by instruments of the permanent seismic and strong motion networks of Greece. In addition, several S-P times determined from digital strong motion records were also taken into account. Four P arrivals, three S arrivals and eleven S-P arrivals were finally used for the mainshock hypocenter determination. The velocity model adopted (Table 1) is based in previous 3-D models, which are valid for the broader Aegean area (Papazachos and Nolet, 1997), with the addition of low-velocity layers for the uppermost crust, in agreement with recent results concerning the studied area (Tselentis and Zahradnik, 2000).

Table 1. Velocity model adopted for the mainshock focal parameters determination.

Depth (km)	V_p (km/s)	V_s (km/s)
0	3.0	1.69
0.9	5.5	3.09
6	6.0	3.37
15	6.5	3.65
31	7.9	4.44

It has to be noted though, that this model is not necessarily representative of the crustal structure in the vicinity of the epicentral area, as it will be shown later. However, it was considered as appropriate for the broader area of interest, despite the fact that no specific station corrections for the P_g and S_g waves were available for the sites of the recording instruments.

The mainshock focal parameters were determined by using the HYPOINVERSE Y2K computer code (Lahr, 1999). The mainshock occurred on September 7, 1999 (11:56:51.4 GMT) with epicentral coordinates $\varphi_N=38.059^\circ$, $\lambda_E=23.571^\circ$ and a focal depth 14.5km. The RMS, ERH and ERZ errors are 0.3 sec, 1.7 Km and 2.3 Km respectively, while the maximum azimuthal gap is of the order of 75° . Figure 1 shows the determined epicenter of the mainshock along with its fault plane solution deduced by Harvard (strike= 114° , dip= 45° , rake= -73°), which suggests an almost normal fault

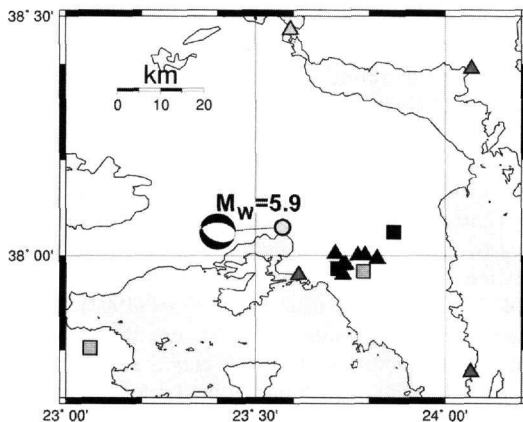


Figure 1. Epicenter of the Athens 1999/9/7, $M_w=5.9$ mainshock. Squares denote stations with P_g or S_g arrivals, while triangles denote stations with P_g-S_g traveltimes.

1. Dept. of Geophysics, School of Geology, Aristotle University of Thessaloniki, PO Box 352-1, Thessaloniki, GR-54006, GREECE
 2. Inst. of Seismology & Earthquake Engineering, PO Box 53, Finikas, Thessaloniki, GR-55102, GREECE

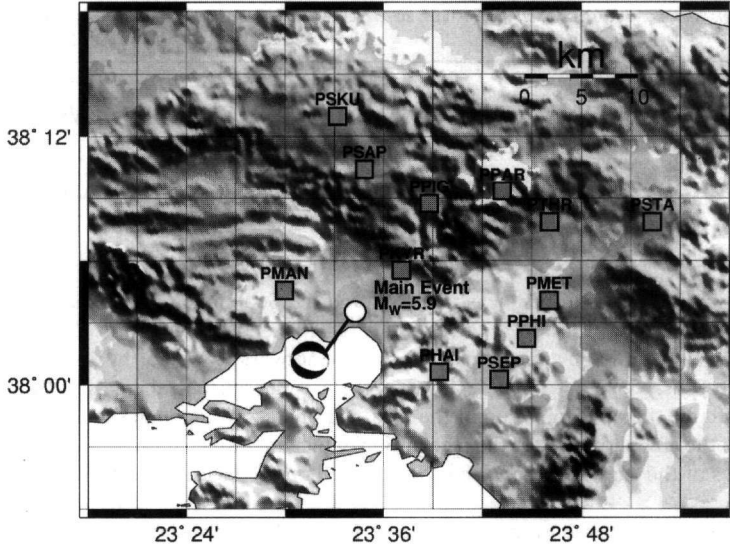


Figure 2. Temporary installation sites (squares) of the seismographs deployed by the Dept. of Geophysics of the Thessaloniki Univ. The main event epicenter and fault plane solution are also shown.

striking WNW-ESE, in agreement with the predominant stress field in the back-arc Aegean area (Papazachos and Kiratzi, 1996).

2. DEPLOYMENT OF PORTABLE INSTRUMENTS IN THE EPICENTRAL AREA

The first portable seismographs (REFTEK) of the Department of Geophysics were installed at the epicentral area two days after the mainshock. Shortly after the preliminary hypocentral determination of the first few aftershocks, which roughly defined the epicentral area, some of the instruments were deployed at new recording sites in order to achieve a better azimuthal coverage with respect to this area. This task inevitably led to the installation of several instruments at sites with relatively high noise level. The final configuration of the temporary network is shown in figure 2, where the installation sites are denoted by squares.

3. DATA ANALYSIS

During the period 11-24 September 1999, when the network was fully operational, 1251 earthquakes were recorded by at least four stations. Their focal parameters were initially determined by the HYPOINVERSE Y2K code (Lahr, 1999), using the velocity model of Table 1. Focal parameters for several relatively strong events, which occurred until October 18, 1999, for which strong motion data had been acquired, were also determined.

Table 2. Final velocity model determined for the aftershock area, adopted for the relocation of the aftershock sequence.

Depth (km)	V_p (km/s)	V_s (km/s)
0	5.08	2.85
1	5.24	2.94
2	5.53	3.11
5.5	6.23	3.50
8	6.28	3.64
10.5	6.51	3.66

In order to refine the hypocentral distribution, which could clearly be improved by a better velocity model and appropriate station corrections, we applied the joint-inversion of travel times for the simultaneous determination of 1-D velocity model and hypocentral locations. The inversion was performed using two independent programs, namely VELEST (Kissling et al., 1995) and a non-linear inversion code (TOMOMEM) by Papazachos and Nolet (1997). Both programs gave very similar results. For the velocity model determination only 204 events that had been

recorded by almost all stations were used, since such events have a negligible effect on the final velocity model. Moreover, appropriate station corrections were estimated from the travel-time inversion process. The final velocity model, which was used for the aftershock relocation is shown in Table 2.

For the study of the main characteristics of the aftershock sequence only high quality relocated aftershocks

have been used. For this reason, only events with at least 7 arrivals, RMS less than 0.25sec and hypocentral error less than 2km have been accepted. The fulfillment of the previous criteria resulted in a final data set of 756 aftershocks, which are studied in the next section.

4. SPATIAL DISTRIBUTION OF THE AFTERSHOCK SEQUENCE

In figure 3a the epicenters of the 756 aftershocks, which have been reliably determined, are presented. The epicenters are located mainly at the central and eastern Thriasion area, between the mountain of Aegaleo, south of mount Parnis and east of the town of Mandra. The determined mainshock epicenter is located close to the Elefsina bay, at the southwesternmost border of the aftershock sequence. The epicenter distribution clearly shows a high concentration of the aftershock activity between the mountains Aegaleo and Parnis, which can be considered as a strong barrier of the rupture zone, where most of the aftershock activity was concentrated.

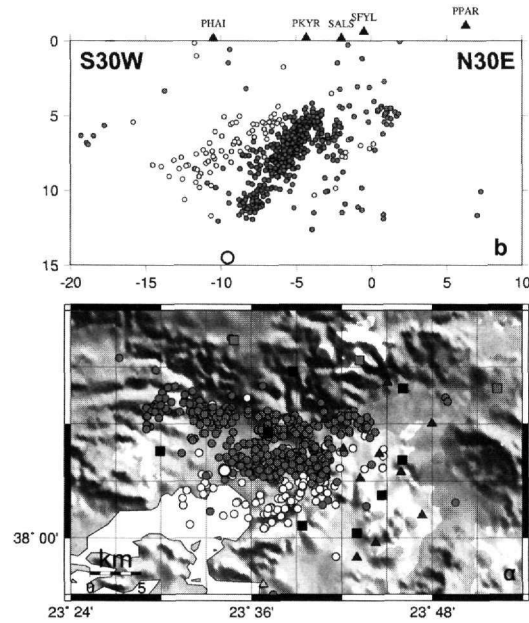


Figure 3. Aftershocks (grey circles) and main event (large open circle) of the 1999/9/7 event. Squares denote stations of the aftershock network, while triangles denote strong motion instruments.

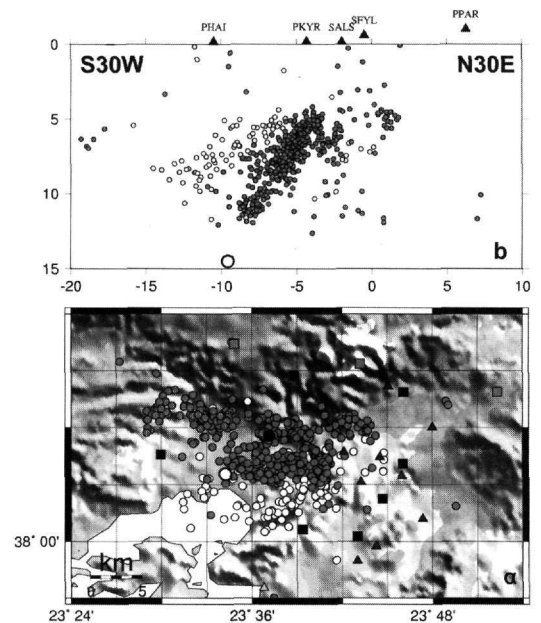


Figure 4. Aftershocks (open circles) which occurred on the 15th and 16th of September (until 15:00) and aftershocks after the 16th of September (15:00) (grey circles). The main event of the 1999/9/7 event is shown with a large open circle. Notice the activation of secondary faults, south of the main fault plane.

The spatial distribution of the aftershocks is also seen in figure 3b where the aftershock hypocenters are projected along a N30°E trending vertical plane, using the point (38.1°N, 23.7°E) as a reference point. The selected projection direction is based on the fault-plane solution, as well as on the results of the analysis presented later. Most of the events have taken place along a SW dipping zone (average slope 45°), towards the Elefsina bay. The main event is located at the deepest section of this zone, although its focal depth seems to be overestimated, as the mainshock is located deeper than its deepest aftershocks (12km), probably due to the poor quality of the regional phase data.

In order to study the spatial distribution of the events, we studied the temporal variation of the seismicity. In general, the aftershock activity seems to deviate from the main fault towards the SW until the noon of 16th of September. This activation of secondary faults in the hanging wall of the fault is clearly seen in figure 4, where the epicenter distribution for the period 15-24 September is shown. Epicenters between the 15th and the 16th of September (until 15:00) are denoted with open circles, while epicenters after the 16th of September (15:00) are denoted with grey circles. Two separate and clearly distinguishable rupture zones are recognized. As we get closer to the noon of 16th September, the seismicity migrated closer to the main fault, where it remains thereafter. This migration is not a result of e.g. problematic locations, etc. since the monitoring network had its final

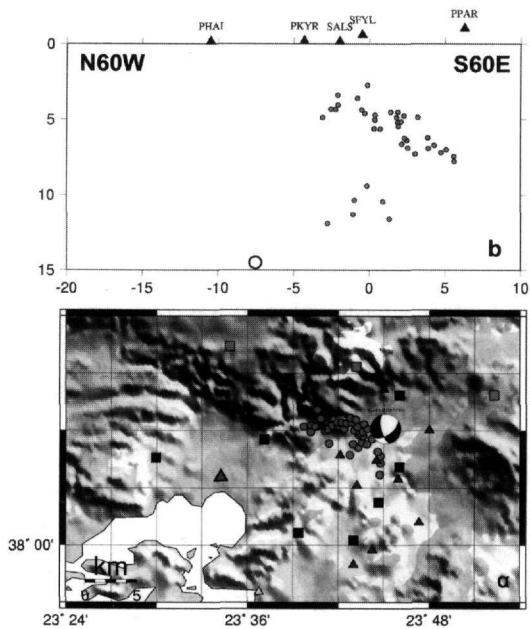


Figure 5. Aftershocks of the Menidi-Liosia-Thrakomakedones area, showing secondary fault activation.

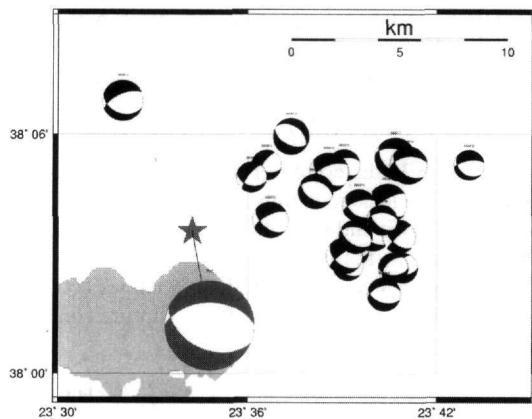


Figure 6. Fault plane solutions determined for selected aftershocks of the Athens sequence. The main event Harvard CMT solution is also plotted, showing a very good agreement between the main event and the aftershocks faulting pattern.

configuration after the noon of the 15th of September, 24 hours before the observed change of seismicity pattern.

The aftershock epicenters which occurred after the noon of the 16th of September delineate a narrow SW dipping rupture zone with a dipping angle of 47°, which is in excellent agreement with the fault-plane solutions and which practically describes the main fault zone. However, it should be noted that several other minor faults had also been activated at the same time. An example is shown in figure 5a where separate seismicity activation is seen in the Menidi-Thrakomakedones area. Figure 5b shows a N120°E section (normal to the previous ones), which clearly shows a second SE dipping fault at the eastern border of the Parnis mountain, in very good agreement with the fault plane solution of largest aftershock in this area (3 October, $M=4.0$), also shown in figure 5a. In the same area, Kontoes et al. (2000) on the basis of interferometer data have suggested the existence of a smaller main-fault segment, corresponding to a $M_w=5.2$ event. Strong motion data (Theodulidis et al., 2000) do not show evidence for a double or multiple rupture. However, the occurrence of several strong aftershocks after the main event along this fault segment can probably explain the high aftershock concentration, as well as the interferometer data.

Figure 6 shows the fault plane solutions determined using more than 5 first motion patterns obtained by the aftershock network. The small number of recording stations, as well as the high noise level at several stations did not allow the computation of a large number of fault plane solutions for the aftershock sequence. In general, the determined fault plane solu-

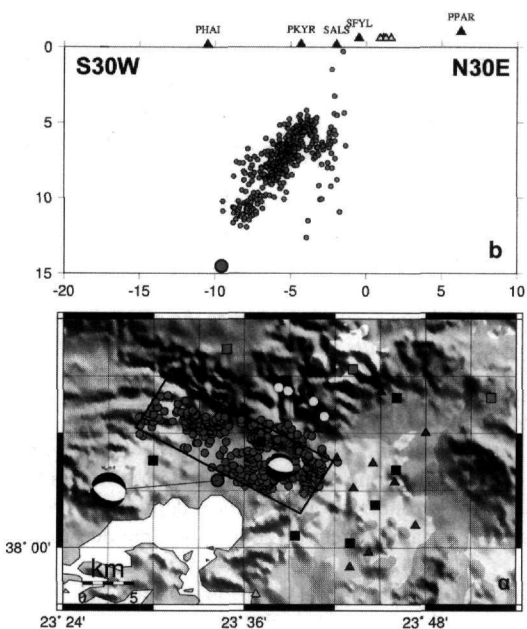


Figure 7. Aftershocks delineating the main fault plane. A typical aftershock fault plane solution, similar to that of the main event is also shown. Open circles in (a) and triangles in (b) denote surface fault traces, located approximately at the surface fault projection.

tions show normal faulting with an average azimuth of 100-130°, which is excellent agreement with the azimuth of 115° of the Harvard solution for the main event, as well as aftershock sequence strike determined in this study.

5. AFTERSHOCK SEQUENCE AND THE MAIN FAULT PLANE OF THE ATHENS EVENT - DISCUSSION

Figure 7a shows the most accurate epicenters of the aftershock sequence that correspond to the main fault. The epicenters define a WNW-ENE trending fault zone, which is delineated by a solid line. The zone length is 18km, in very good agreement with the predicted length of 15km based on the event magnitude ($M_w=5.9$) using the relation of Papazachos and Papazachou (1997), as well as from results based on waveform modeling (e.g. Papadimitriou et al., 2000; Tselentis and Zahradnik, 2000). The mainshock epicenter position is at the deepest central section of the fault, similarly to many other events in the broader Aegean area (e.g. Kozani 1995 sequence, Papazachos et al., 1998). Most aftershocks are found on the eastern fault segment (closer to Athens) that, if accurate due to the uneven network distribution, permits the determination of high- and low-slip fault segments during the main rupture.

The direction of the aftershock sequence (120°) is in very good agreement with the surface ruptures at the Parnis mountain area, which are presented in figure 7a with open circles. A similar fault strike has been determined by the Harvard CMT solution. Almost all events have occurred between the depths of 4-12km, along a zone which dips at an angle of 45-50°, towards the Elefsina bay. The main event hypocentral depth estimated here is probably slightly overestimated, as can be inferred by the maximum aftershock depth, which is probably due to the limited amount of regional P_g and S_g phase data. In any case, the hypocenter corresponds to the initiation rupture point, while the center of energy release has been shown to occur at the depth of 8km (Papadimitriou et al., 2000; Tselentis and Zahradnik, 2000, Theodulidis et al., 2000). Therefore, the rupture must have started from the depth of 12km and propagated upwards up to the depth of 4km, where it stopped.

The results obtained in the present study are in good agreement with previous results about the aftershock sequence of the Athens event. The aftershock distribution determined in the present work is clearly delineating the main fault, in comparison with the results of other previous studies (e.g. Papadopoulos et al., 2000), which show a very poor control of focal depths and description of the fault plane, probably due to the use of analog recordings. Furthermore, the obtained results are show an excellent correlation with the results of Voulgaris et al. (2000), both in the aftershock distribution, as well as in their density along the fault. In addition, in the present study we were able to map secondary faults (see figure 4 and 5) that were activated during the aftershock sequence.

A lot of discussion has taken place concerning the active tectonic fault to which this event should be attributed. Papadopoulos et al. (2000) have suggested that the rupture zone lies on the possible Fyli fault, already identified by Galanopoulos (1967), which runs parallel and to the north of the major Thriasion basin fault. This can also be seen in figure 8 where the aftershock epicenters have been aligned along the possible fault plane continuation towards the surface, showing a very good correlation with the possible Fyli fault. However, we believe that such a correlation is slightly exaggerated as all seismic activity is confined at depths larger than 4km. Therefore, the identified fault is a typical "hidden" fault with no surface projection, similarly to many other similar magnitude events in Greece (e.g. Patras, 1993; Kozani, 1995). In these cases it is not only difficult but also quite risky to attempt a correlation of the "hidden" seismic fault with surface fault traces, as there is no clear way to extrapolate the fault trace towards the surface, since the fault might be either planar or listric as has been shown to apply for many faults at basin borders. As can be seen (e.g. from figure 4) one could easily extrapolate the hypocentral distribution towards the surface in a listric sense, as with many observed neotectonic faults which are sub-vertical at the surface, so that it reaches the surface slightly north of station PKYR, therefore coinciding with the Thriasion and not the Fyli fault. Similar conclusions have been pointed out by other researchers (Voulgaris et al., 2000), which also observed some along-strike variations of the fault dip. Furthermore, the identified surface displacements (Papadopoulos et al., 2000) along the area of the proposed Fyli fault are too small to be clearly associated with the surface continuation of the fault. For these reasons, we believe that there is no need to arbitrarily extrapolate the fault-plane towards the surface in order to correlate it with the Fyli fault and that we should simply consider the Athens earthquake as an event which is due to a "hidden" normal fault located between the depths of 4 and 12km.

ACKNOWLEDGEMENTS

This work is a Department of Geophysics, Univ. of Thessaloniki contribution number #553/2001.

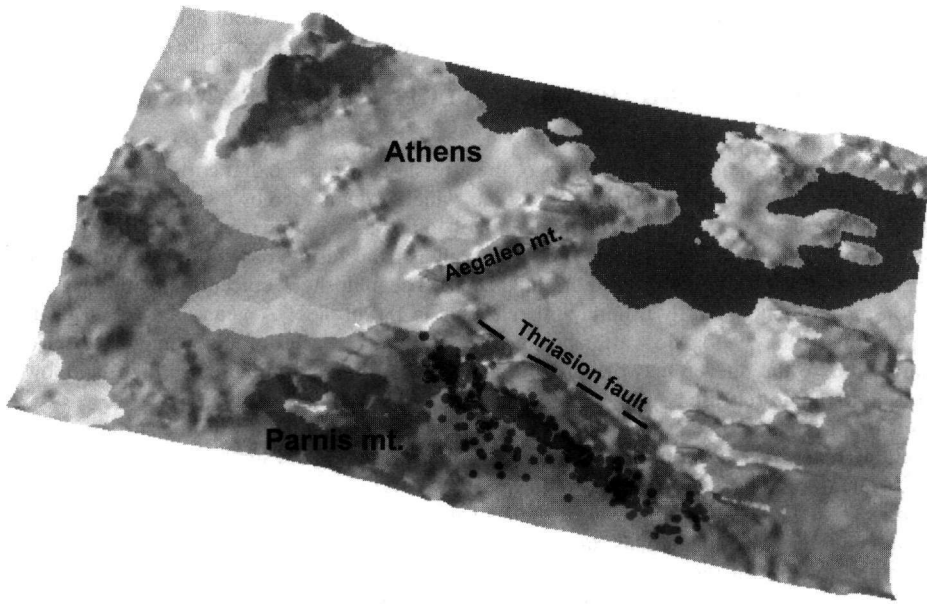


Figure 8. Projection of the main fault-plane aftershocks on a semi-transparent morphological background. The projection is chosen in order to align the aftershock projections along the projected fault-plane surface. Notice that the surface projection does not coincide with the Thriasian basin fault.

REFERENCES

- GALANOPOULOS, A. G. 1967. The influence of the fluctuation of the Marathon lake elevation on local earthquake activity in the Attica basin area, *Annales Geologiques des Payes Helleniques* 18, 281-306.
- KISSLING, E., KRADOLFER, U., AND MAURER H., VELEST user's guide, ETH Zurich, Institute of Geophysics, 22pp.
- KONTOES, C. , BRIOLE, P., SACHPAZI, M. , VEIS, G., ELIAS, P., KOTSIS, I. , SYKIOTI, O., REMY, D. 2000. Displacement field mapping and fault modelling of the Mw=5.9, September 7, 1999 Athens earthquake based on ERS-2 satellite radar interferometry, *Geoph. Res. Let.* 27, 3989-3992.
- LAHR, J. C. 1999. HYPOELLIPSE: A Computer Program for Determining Local Earthquake Hypocentral Parameters, Magnitude and First-Motion Pattern (Y2K Compliant Version), *U.S.Geological Survey Open-File Report 99-23*.
- PAPADIMITRIOU, P., KAVIRIS, G., VOULGARIS, N., KASSARAS, I., DELIBASIS, N., AND MAKROPOULOS, K. 2000. The September 7, 1999 Athens earthquake sequence recorded by the CORNET network: Preliminary results of source parameters determination of the mainshock. *Annales Geologiques des Payes Helleniques* 38, 29-40.
- PAPADOPOULOS, G. A., DRAKATOS, G., PAPANASTASSIOU, D., KALOGERAS, I., AND STAVRAKAKIS, G. 2000. Preliminary results about the catastrophic earthquake of the 7 September 1999 in Athens, Greece, *Geophys. Res. Let.* 71, 3, 318-329.
- PAPAZACHOS, B. C., AND PAPAACHOU, C. C. 1997. The earthquakes of Greece, *Ziti Publ.*, Thessaloniki, 304pp.
- PAPAZACHOS, B. C., KARAKOSTAS, B. G., KIRATZI, A. A., PAPADIMITRIOU, E. E., AND PAPAACHOS, C. B. 1998. A model for the 1995 Kozani-Grevena seismic sequence, *J. Geodynamics* 26, 217-231.
- PAPAZACHOS, C. B., AND KIRATZI, A. A. 1996. A detailed study of the active crustal deformation in the Aegean and surrounding area, *Tectonophysics* 253, 129-153.
- PAPAZACHOS, C. B., AND NOLET, G. 1997. P and S deep velocity structure of the Hellenic area obtained by robust non-linear inversion of travel times, *J. Geophys. Res.* 102, 8349-8367.
- THEODULIDIS, N., MARGARIS, B.N., PAPAIOANNOU, CH., AND DIMITRIOU, P. 2000. Preliminary report on the strong motion as selected sites of the meioseismic area of NW Attica during the event of 7/9/1999, Technical Report.
- TSELENTIS, G-A., AND ZHRADNIK, J. 2000. Aftershock monitoring of the Athens earthquake of 7 September 1999, *Geophys. Res. Let.* 71, 3, 330-337.
- VOULGARIS, N., KASSARAS, I., PAPADIMITRIOU, P., AND DELIBASIS, N. 2000. Preliminary results of the Athens September 7, 1999 aftershock sequence. *Annales Geologiques des Payes Helleniques* 38, 29-40.